

Aluminum Magadiite: an Acid Solid Layered Material

Guilherme B. Superti, Erica C. Oliveira, and Heloise O. Pastore*

*Instituto de Química, Universidade Estadual de Campinas, CP 6154,
CEP 13083-971, Campinas, SP, Brasil*

Alessandro Bordo, Chiara Bisio, and Leonardo Marchese*

*Nano-SISTEMI Interdisciplinary Centre, DISTA, University of Eastern Piedmont “A. Avogadro”,
via G. Bellini 25G, 15100, Alessandria, Italy*

Received March 20, 2007. Revised Manuscript Received June 5, 2007

Aluminum-modified magadiite samples with high concentration of aluminum have been synthesized under hydrothermal conditions by modifying the traditional preparation route of the layered siliceous material. A new synthetic strategy, named aluminum-induced crystallization (AIC) method, was thus developed to introduce different amounts of Al in the siliceous framework. A systematic study of the physicochemical properties and thermal behavior of the produced Al-derived magadiite materials was performed by combining different experimental techniques [infrared spectroscopy (IR) of adsorbed probe molecules, X-ray diffraction (XRD), thermogravimetric analysis (TGA), and solid-state magic-angle spinning nuclear magnetic resonance (SS MAS NMR)]. ²⁷Al SS MAS NMR showed that the synthesis method allowed us to introduce for the first time Al ions in a magadiite framework in tetrahedral positions. Variable-temperature XRD analysis showed that the introduction of Al in tetrahedral position does not affect the thermal stability of the silica layers. The presence of Al ions led to a modification of the surface acidity of magadiite. Indeed, Fourier transform infrared (FTIR) measurements of CO adsorbed at 100 K indicated the presence of Brønsted acidity similar to that found in highly acidic zeolites. The amount of acid sites is progressively increased by introducing increasing amounts of Al in the framework. Moreover, different families of Brønsted acid sites with different acid strengths are present at higher Al content, thus revealing the possibility to tune the surface acidity of these materials.

Introduction

Hydrated layered silicates and silicic acids are extremely versatile materials. Magadiite, kenyaite, kanemite, and ilerite have been used after organosilylation as adsorbents^{1–3} and as sources of new layered materials, FLS and KLS 1–3, with improved porosity properties;^{4–7} their interlayer galleries also have been used for enzyme immobilization.⁸

Silica-pillared H kanemite,⁹ H magadiite,^{10,11} H kenyaite,¹² H ilerite,¹³ and mixed-oxide pillared H ilerite¹⁴ were prepared by simultaneous reaction with tetraethoxysilane and octyl-

or dodecylamine and displayed mesoporosity. As a matter of fact, the first mesoporous silica material FSM-16, antecedent of MCM-41, was prepared from hexadecyltrimethylammonium intercalated kanemite.¹⁵ Pillared materials are interesting and useful solids since the size of the pores is believed to be controlled by the size of the pillars,^{1,16} which can be made by design, and can cover the gap from micro- to mesoporous materials.¹⁷

These layered hydrated silicates were also used as reactants in the synthesis of zeolites by recrystallization processes. ZSM-5,^{18–22} -11,²² -12,^{19–21} -35,^{19–21} -39^{19–21} and -48^{19–21} were all prepared starting from magadiite, as well as EU-2,^{19–21} FU-1,^{19–21} SSZ-15,^{19–21} and mordenite.²⁸

Kanemite was used to prepare silicalites 1^{23–28} and 2.²⁴ Schwieger and co-workers²⁹ reported the transformation of kanemite into β -zeolite upon hydrothermal transformation in the presence of various concentrations of aluminum. Although SiO₂/Al₂O₃ molar ratios indicated high concentrations of aluminum in the solid product, pure β -zeolites were

* Corresponding authors: e-mail (H.O.P.) gpmmm@iqm.unicamp.br or (L.M.) leonardo.marchese@mf.unicamp.br

- (1) Sprung, R.; Davis, M. E.; Kauffman, J. S.; Dybowski, C. *Ind. Eng. Chem. Res.* **1990**, *29*, 213.
- (2) Thiesen, P. H.; Beneke, K.; Lagaly, G. *J. Mater. Chem.* **2002**, *12*, 3010.
- (3) Fujita, I.; Kuroda, K.; Ogawa, M. *Chem. Mater.* **2003**, *15*, 3134.
- (4) Kooli, F.; Kiyozumi, Y.; Mizukami, F. *New J. Chem.* **2001**, *25*, 1613.
- (5) Kooli, F.; Mizukami, F.; Kiyozumi, Y.; Akiyawa, Y. *J. Mater. Chem.* **2001**, *11*, 1946.
- (6) Kooli, F.; Kiyozumi, Y.; Rives, V.; Mizukami, F. *Langmuir* **2002**, *18*, 4103.
- (7) Kooli, F. *J. Mater. Chem.* **2002**, *12*, 1374.
- (8) Peng, S.; Gao, Q.; Wang, Q.; Shi, J. *Chem. Mater.* **2004**, *16*, 2675.
- (9) Toriya, S.; Tamura, Y.; Takei, T.; Fuji, M.; Watanabe, T.; Chikazawa, M. *J. Colloid Interface Sci.* **2002**, *255*, 171.
- (10) Jeong, S.-Y.; Kwon, O.-Y.; Suh, J.-K.; Jing, H.; Lee, J. M. *J. Colloid Interface Sci.* **1995**, *175*, 253.
- (11) Kwon, O.-Y.; Shin, H.-S.; Choi, S.-W. *Chem. Mater.* **2000**, *12*, 1273.
- (12) Jeong, S.-Y.; Suh, J.-K.; Jin, H.; Lee, J.-M.; Kwon, O.-Y. *J. Colloid Interface Sci.* **1996**, *180*, 269.
- (13) Kosuge, K.; Tsunashima, A. *J. Chem. Soc., Chem. Commun.* **1995**, 2427.
- (14) Kosuge, K.; Sing, P. S. *Chem. Mater.* **2000**, *12*, 421.

- (15) Yanagisawa, T.; Shimizu, T.; Kuroda, K.; Kato, C. *Bull. Chem. Soc. Jpn.* **1990**, *63*, 1535–7.
- (16) Fetter, G.; Tichit, D.; Massiani, P.; Dutartre, R.; Figueras, F. *Clays Clay Miner.* **1994**, *42*, 161.
- (17) Galarneau, A.; Barodawalla, A.; Pinnavaia, T. J. *Nature* **1995**, *374* (6522), 529.
- (18) Hogan, P. J. U.K. Patent Appl. 2,125,390A, 1983.
- (19) Zones, S. I. U.S. Patent 4,626,421, 1986.
- (20) Zones, S. I. U.S. Patent 4,676,958, 1987.
- (21) Zones, S. I. U.S. Patent 4,689,207, 1987.
- (22) Pal-Borbély, G.; Beyer, H. K.; Kiyozumi, Y.; Mizukami, F. *Microporous Mater.* **1997**, *11*, 45.

obtained only in high-silica gels. Larger quantities of aluminum in the gels led to the formation of mordenite as contaminating phase.

Ferrierite was also prepared from kanemite by a solid-state synthesis.³⁰ In the process, the kanemite was transformed to an amorphous material as, differently from magadiite (see below), it is thermally unstable.

Metal-substituted zeolites can also be prepared by this method. Manganese ion-exchanged magadiite was recrystallized in a tetrapropylammonium hydroxide solution into Mn-MFI metallosilicate. Scanning electron microscopy showed that the samples were composed of very homogeneous elongated prismatic crystals, 20–30 μm in length, typical of ZSM-5.³¹

Ferrierite was prepared by recrystallization of magadiite in the presence of piperidine³² by a method that did not require the addition of water, the dry method. Unfortunately, cation-exchange capacity measurements indicated that part of the aluminum present in magadiite was not transported to the ferrierite framework, although the analysis of bulk aluminum showed the presence of the totality of this element.

This might pose a problem when controlled Al levels are desired in the final product, especially because the preparation of zeolites from hydrated layered silicates affords crystals with unusual morphologies, some of them displaying larger access to the internal part of the crystals and to catalytic sites. It would be highly desirable to have better control of the Al concentration on the crystals and their localization, to make designed acidity possible. In that sense, a better understanding of what the layered [Al] magadiite precursor is and how to prepare it with improved properties is one starting point. In that direction, only two works were found in the literature^{33,34} that involved the preparation and an incipient characterization of Al magadiite. In one of these works, the aluminum incorporated in the magadiite was present as an impurity of water glass; no further Al was externally added.³³ In the other work,³⁴ the amount of aluminum incorporated in the magadiite structure varied from $\text{SiO}_2/\text{Al}_2\text{O}_3$ 23 to 360; that is, the material could incorporate larger amounts of aluminum, but in that case, the synthesis times could be as large as 20 days.

This paper is dedicated to describing a method to prepare [Al] magadiite with larger concentrations of aluminum incorporated into the layered framework. The physicochemical properties of these materials will also be discussed, with special emphasis on their acidity and thermal behavior. Toward this aim, a systematic study of the [Al]-modified magadiite samples was carried out by using spectroscopic tools and by studying the materials under controlled conditions of temperature and pressure. To our knowledge, this is the first study of the surface properties of [Al] magadiite samples monitored by IR of probe molecules, supported also by thermogravimetric analysis (TGA) and X-ray diffraction (XRD) studies.

Experimental Section

Synthesis of Magadiite (Na Magadiite). Sodium metasilicate (1.77 mol, Nuclear) was dissolved in distilled water (31.80 mL) and the pH was adjusted between 10.78 and 10.82 with concentrated HNO_3 (Merck, 63%). The gel was aged for 4 h at 347–349 K and then transferred to a stainless steel autoclave lined with Teflon for the hydrothermal treatment for 66 h at 423 K. After that, the sample was filtered and washed with distilled water until neutral pH and dried in air.

Synthesis of Aluminum Magadiite (Na[Al] Magadiite). Two methods were used for this synthesis:

(1) *Direct Method.* Sodium metasilicate (1.77 mol, Nuclear) was dissolved in distilled water (31.80 mL), and aluminum isopropoxide (1.89 mmol, Alfa Aesar) was added. After hydrolysis of the aluminum source, the pH was adjusted in the range 10.78–10.82 with concentrated HNO_3 (Merck, 63%). The gel thus formed was aged for 4 h, heated at 347–349 K, and transferred to a stainless steel autoclave lined with Teflon for 66 h at 423 K.

(2) *Aluminum-Induced Crystallization Method.* This method is similar to the one already described. A gel, prepared as for the synthesis of magadiite, was pretreated at 423 K for 12 or 24 h. After this time, aluminum isopropoxide was added (3.78, 1.89, and 0.95 mmol for Si/Al 15, 30, and 60, respectively). The autoclave was closed and heated at the same temperature for another period of 12, 24, or 48 h.

In both methods the obtained materials were washed with distilled water until pH 7 and dried in air. The samples were named 15[Al], 30[Al], and 60[Al] magadiite for Si/Al 15, 30, and 60, respectively.

For the determination of acid sites, each sample was exchanged with an $0.1 \text{ mol}\cdot\text{L}^{-1}$ NH_4Cl solution (5 g of magadiite/L of solution) at room temperature for 24 h under magnetic stirring. After that, the solids (hereafter named NH_4 -[Al] magadiite) were filtered and washed until they tested negative for chloride. This process was repeated three times. A sample of purely siliceous Na magadiite was also exchanged by the same procedure and named NH_4 magadiite. The proton-exchanged [Al] magadiite was prepared by preparing a suspension of 15 g of Na magadiite in 500 mL of distilled water to which HCl $0.1 \text{ mol}\cdot\text{L}^{-1}$ was added until $\text{pH} = 1.9$. The suspension was stirred at room temperature for 24 h. The solid was filtered and washed with copious amounts of distilled water until it tested negative for chloride.

- (23) Kiyozumi, Y.; Salou, M.; Mizukami, F. *Stud. Surf. Sci. Catal.* **2002**, *142A*, 2.
- (24) Salou, M.; Kiyozumi, Y.; Mizukami, F.; Nair, P.; Maeda, K.; Niwa, S. *J. Mater. Chem.* **1998**, *8*, 2125.
- (25) Salou, M.; Kiyozumi, Y.; Mizukami, F.; Nair, P.; Maeda, K.; Niwa, S. *Mol. Cryst. Liq. Cryst. Sci. Technol., Sect. A* **1998**, *322*, 141.
- (26) Salou, M.; Kiyozumi, Y.; Mizukami, F.; Kooli, F. *J. Mater. Chem.* **2000**, *10*, 2587.
- (27) Ko, Y.; Kim, M. H.; Kim, S. J.; Uh, Y. S. *Korean J. Chem. Eng.* **2001**, *18*, 392.
- (28) Shimizu, S.; Kiyozumi, Y.; Maeda, K.; Mizukami, F.; Pál-Borbély, G.; Magdolna, R.; Beyer, H. K. *Adv. Mater.* **1996**, *8*, 759.
- (29) Selvam, T.; Baudarapu, B.; Mabaude, G. T. P.; Toufar, H.; Schwieger, W. *Microporous Mesoporous Mater.* **2003**, *64*, 41.
- (30) Pál-Borbély, G.; Szegedi, A.; Beyer, H. K. *Microporous Mesoporous Mater.* **2000**, *35–36*, 573.
- (31) Ko, Y.; Kim, S. J.; Kim, M. H.; Park, J.-H.; Parise, J. B.; Uh, Y. S. *Microporous Mesoporous Mater.* **1999**, *30*, 213.
- (32) Pál-Borbély, G.; Beyer, H. K.; Kiyozumi, Y.; Mizukami, F. *Microporous Mesoporous Mater.* **1998**, *22*, 57.
- (33) Pál-Borbély, G.; Auroux, A. *Stud. Surf. Sci. Catal.* **1995**, *94*, 55.
- (34) Schwieger, W.; Pohl, K.; Brenn, U.; Fyfe, C. A.; Grondy, H.; Fu, G.; Kokotailo, G. T. *Stud. Surf. Sci. Catal.* **1995**, *94*, 47.

Characterization Techniques: X-ray Powder Diffraction. Solids were measured with the aid of a Shimadzu XRD-6000, with Cu K α radiation (40 kV, 30 mA), at a scan rate of 2° 2 θ min⁻¹, at room temperature from pressed powders, and at increasing temperatures at ambient atmosphere. Crystallinity degrees were calculated by integrating the area under the peaks between 22° and 30° 2 θ ; all samples were compared to the most crystalline one.

Variable-temperature diffractograms (VT-XRD) were obtained both on the Shimadzu described above and on a ARL X'TRA diffractometer, this last operating at the same conditions as the Shimadzu. The attachments for VT-XRD were (a) a Shimadzu heating accessory, model HA101, under both nitrogen and air and (b) a Buelher high-temperature stage under nitrogen. The results of Na magadiite and NH₄ magadiite obtained with the Shimadzu accessory and those of NH₄[Al] magadiite obtained with the Buelher accessory are presented here. The samples were heated at a rate of 5 K·min⁻¹ and left to equilibrate at each temperature for 15 min, before the diffractograms are registered (more than 60 min scan).

Fourier Transform Infrared Spectra. IR spectra were collected on a Bruker Equinox 55 spectrometer equipped with a DTGS detector (resolution 4 cm⁻¹). All gases employed in the adsorption–desorption experiments were high-purity grade. CO was admitted on the samples by passage through a trap cooled down to liquid nitrogen temperature.

The samples were pressed in the form of self-supporting wafers (with a pressure of 5 tons/cm²) and placed into a IR cell equipped with KBr windows permanently attached to a high-vacuum line (residual pressure 1.0 × 10⁻⁵ Torr; 1 Torr = 133.33 Pa), allowing all treatments and adsorption–desorption experiments to be carried out in situ.

NH₄[Al] magadiite samples were heated from room temperature (rt) to 623 K (5 K/min) under high dynamic vacuum prior to the adsorption of probe molecules, kept at this temperature for 3.5 h, and then cooled down to rt. This treatment was necessary to decompose and remove the NH₄⁺ ions in exchange positions, thus activating the acidity of the materials. These samples were named H[Al] magadiite. The NH₄ magadiite sample was also decomposed (and named H magadiite) following the same procedure before spectroscopic characterization.

IR spectra of the various samples have been normalized, with the intensity of the overtones and combination modes of the silica framework in the range 2200–1600 cm⁻¹ taken into account. In this way, differences in the intensity of the bands related to intrinsic oscillators of the materials (e.g., hydroxyl groups) or adsorbed on them (probe molecules) can be related to difference in the amount of such species in the samples. As a consequence of the normalization, the absorbance values are reported as arbitrary units (au).

Solid-State Nuclear Magnetic Resonance. Spectra were measured for ²⁷Al and ²⁹Si in a Bruker AC 300/P. The samples were spun at 4.5 kHz in a zirconia rotor. More than 1200 scans were obtained for proton-decoupled ²⁹Si NMR, with 60 s delay time and tetramethylsilane (TMS) as reference. For proton-decoupled ²⁷Al, more than 2000 scans were accumulated at 1 s delay time and an aqueous acid solution of Al(NO₃)₃ was the reference.

Elemental Analyses. The amounts of Na, Al, and Si were determined by atomic absorption spectroscopy (AAS) and

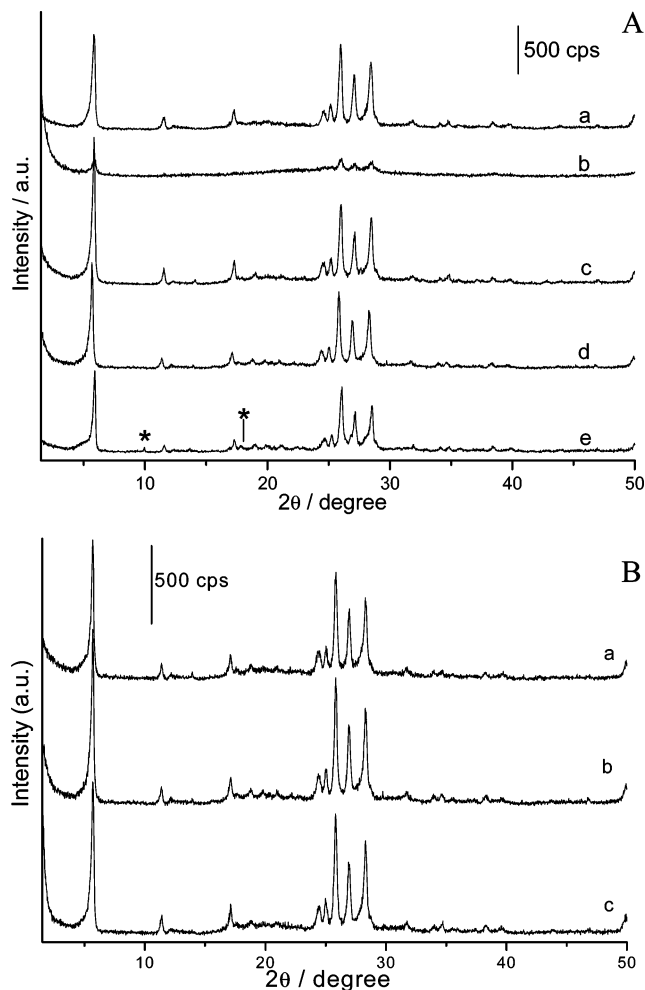


Figure 1. (A) X-ray diffractograms (XRD) of (a) pure siliceous Na magadiite prepared by the method discussed here and of 30[Al] magadiite samples prepared with variable times of pre/final hydrothermal treatments: (b) 12 h/12 h, (c) 24 h/12 h, (d) 24 h/24 h, and (e) 24 h/48 h. Asterisks indicate contamination. (B) XRD of Na[Al] magadiite obtained for different Si/Al ratios by the aluminum-induced crystallization method: (a) Si/Al = 15, (b) Si/Al = 30, and (c) Si/Al = 60 (prepared with the optimum conditions 24 h pretreatment, 12 h posttreatment times).

inductively coupled plasma mass spectrometry (ICP-MS) by ITECON (Nizza Monferrato, Italy) and Puriquima (São Paulo, Brazil) laboratories after an oxidative alkaline fusion procedure. The N content was measured on a Perkin-Elmer CHNS/O atomic analyzer 2400, series II, with approximately 1 mg of sample.

Thermogravimetric Analysis. Measurements were made in a TA Instruments 5100, heating rate 10 K min⁻¹ until 1273 K, under 100 mL min⁻¹ argon flow.

Scanning Electron Microscopy. Samples were coated with carbon and measured in a Jeol 6360-LV, operating at 20 kV.

Results and Discussion

Due to the complexity of the collected spectroscopic data concerning [Al] magadiite samples, an appropriate revisiting of the physicochemical and structural properties of the parent Na magadiite samples was also needed, especially concerning their surface features in relation to the hydration state.

Pure siliceous Na magadiite prepared by the procedures described here showed a characteristic X-ray diffraction (XRD) pattern of the structure reported in the literature^{35,36} (Figure 1A, curve a). This material has a lamellar structure

Table 1. Materials Obtained by Different Hydrothermal Pre- and Posttreatment

Figure 1	hydrothermal		phase (% crystallinity)
	pretreatment, h	posttreatment, h	
curve b	12	12	amorphous + magadiite (39.7)
curve c	24	12	magadiite (100)
curve d	24	24	magadiite (95.4)
curve e	24	48	magadiite + other structure (86.7)

as shown by the typical signals at 5.68° (1.55 nm), 11.36° (0.78 nm), and 17.11° 2θ (0.52 nm), corresponding to (001), (002), and (003) diffraction planes, respectively. Moreover, signals between 23° and 30° 2θ (3.83–2.94 Å) indicate the crystalline nature of the layer.³⁵

The addition of the aluminum source in the initial gel (direct method) resulted in amorphous materials or heavily contaminated magadiite (data not shown) as already pointed out by Schwieger et al.³⁴ Therefore, the aluminum-induced crystallization (AIC) method was developed. Figure 1 shows the XRD of 30[Al] magadiite samples prepared by the AIC method with variable pre- and posttreatment times (curves b–e); the percentages of crystallinity of the various samples are reported in Table 1.

The most crystalline material, without contamination, was obtained with 24 h of treatment before the addition of the aluminum source and 12 h more of hydrothermal treatment at the same temperature after the addition of aluminum (Figure 1A, curve c).

These results indicated that aluminum accelerates magadiite crystallization because analogous pure siliceous magadiite is synthesized with 66 h of total time of hydrothermal treatment.³⁷

Diminishing the time of hydrothermal post- and precrystallization to 12 h caused the appearance of magadiite with lower crystallinity, while increasing the time of the hydrothermal posttreatment either slightly diminished the crystallinity (after 24 h) or led to the formation of extra phases (after 48 h). Therefore, the AIC method with 24 h of hydrothermal pretreatment and 12 h posttreatment was adopted for the preparation of [Al] magadiite with different Si/Al molar ratios. These materials presented X-ray diffractograms characteristic of the magadiite structure (Figure 1B, curves a–c) and showed that the crystallinity does not change significantly by the introduction of aluminum into the silica framework.

Table 2 shows the chemical composition, the Si/Al molar ratios in the gels (Si/Al_(g)), and the Si/Al molar ratio in the solid (Si/Al_(s)).

The concentration of Na⁺ ions increases passing from Na magadiite onto Na[Al] magadiite indicating that Al-derived samples contain a higher amount of negatively charged surface species and that these are counterbalanced by Na⁺

ions. While in pure siliceous magadiite the alkali cations neutralize SiO[−] surface species [as confirmed by Fourier transform infrared (FTIR) data, see later], for Al-derived samples Na cations should act as countercations for both SiO[−] groups and Si(O[−])Al species formed upon Al introduction. The presence of these latter species was confirmed by FTIR and ²⁷Al magic-angle spinning (MAS) NMR (vide infra). The exchange of Na magadiite and Na[Al] magadiite samples in NH₄Cl aqueous media allowed to substitute a large fraction of Na⁺ with NH₄⁺ ions. The exchange procedure is not complete, as indicated by the residual presence of Na⁺ ions in NH₄[Al] magadiite samples.

In addition, it can be noticed that the overall concentration of countercations (NH₄⁺ and Na⁺ ions) is always lower than the Na⁺ amount in parent Na-exchanged samples. This fact suggests that the NH₄⁺-exchanged samples should display more abundant surface Si–OH species, with consequent loss of surface exchange sites. On the basis of chemical analysis, in fact, 75–85% of surface SiO[−] species were lost with respect to Na-exchanged parent samples. Water interaction with SiO[−] species should occur during the ion exchange in aqueous solution, and this leads to the formation of SiOH groups, and consequent loss of surface exchange sites.

The concentration of N atoms in NH₄[Al] magadiite samples deserves some additional comments in that even if the ion exchange is not complete for siliceous and Al-containing magadiite samples, the concentration of Na⁺ ions is always lower than the NH₄⁺ content (Table 2). Interestingly, the concentration of N species increases by increasing the Al content, thus suggesting that variable amount of bridged Si(O[−])Al groups are generated in magadiite samples by properly varying the gel composition. Nevertheless, the fact that the sum of Na⁺ and NH₄⁺ countercations is lower than the Al content suggests that Al₂O₃ aggregates are also formed in parallel to Si–OH surface sites. A higher concentration of surface silanols was, in fact, monitored by IR spectroscopy (data not shown for the sake of brevity).

As far as the Si/Al ratio in ammonium-exchanged samples is concerned, the crystalline products show values similar to those used in the gel synthesis. Nevertheless, after NH₄⁺ exchange the Al concentration decreases, and the Si/Al ratio becomes generally higher than the Si/Al ratio of the synthesis gel. The ion-exchange procedure in acid medium (H[Al] magadiite) leads to a further reduction of Al in the sample, for example, a partial Al leaching occurs, which is accompanied by the formation of surface point defects (silanols), as found by FTIR spectroscopy (see later).

The general morphology of samples is not changed by the presence of aluminum as demonstrated in Figure 2, which shows the scanning electron micrographs of Na magadiite

Table 2. Chemical Composition of Synthetic Magadiite Samples. Values are Referred to Dry Samples.

sample (Si/Al _(g) ratio)	[Na] (mmol·g ^{−1})	[N] (mmol·g ^{−1})	[Al] (mmol·g ^{−1})	[N] + [Na] (mmol·g ^{−1})	Si/Al _(s)
Na magadiite	1.80			1.80	
Na[Al] magadiite (Si/Al = 15)	2.69		1.43	2.69	15
Na[Al] magadiite (Si/Al = 30)	2.90		1.16	2.90	16
NH ₄ magadiite	0.0087	0.45		0.46	
NH ₄ [Al] magadiite (Si/Al = 15)	0.26	0.48	1.19	0.74	20
NH ₄ [Al] magadiite (Si/Al = 30)	0.11	0.31	0.79	0.42	32
NH ₄ [Al] magadiite (Si/Al = 60)	0.057	0.32	0.40	0.37	56
H[Al] magadiite (Si/Al = 30)	0.032		0.39	0.032	69

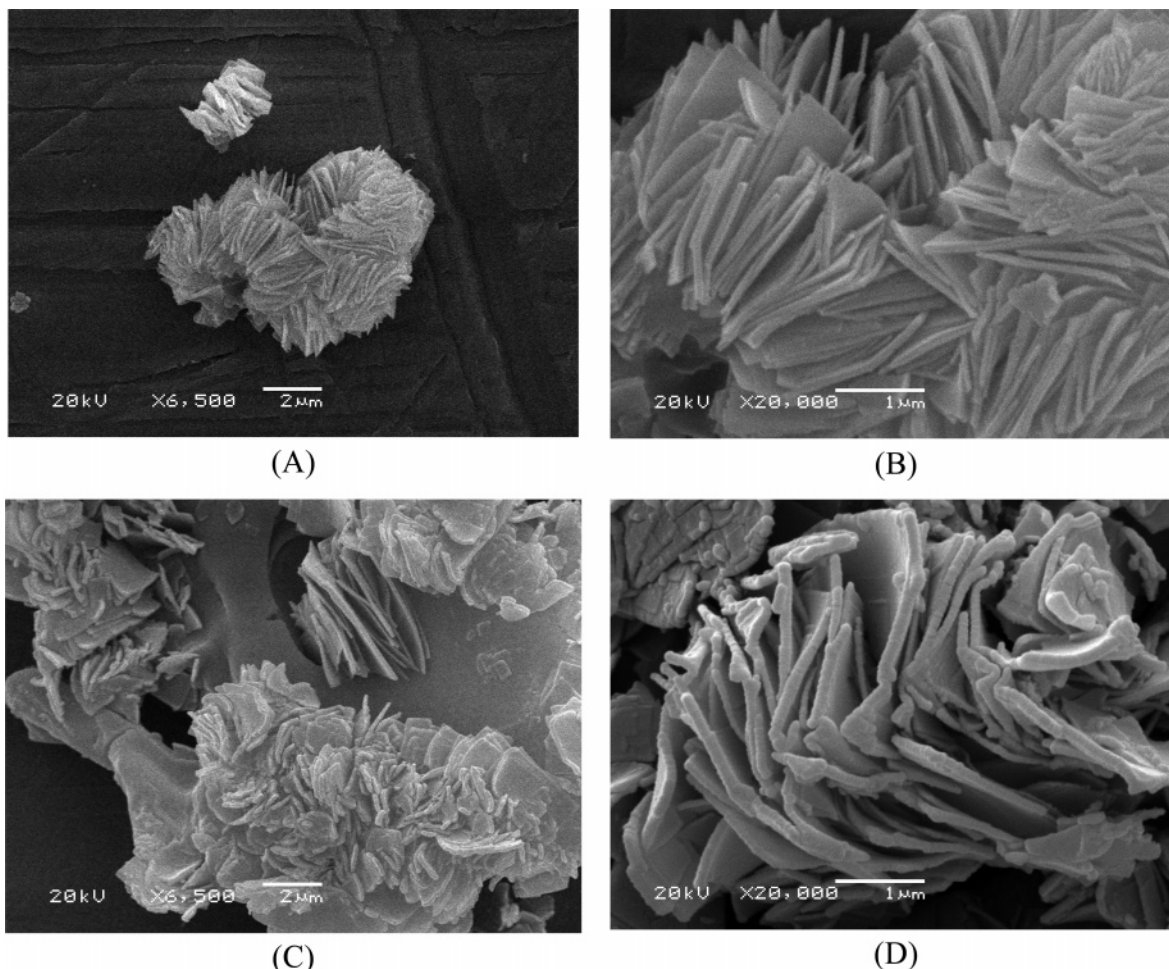


Figure 2. Scanning electron microscopy of (A, B) magadiite and of (C, D) 30[Al] magadiite.

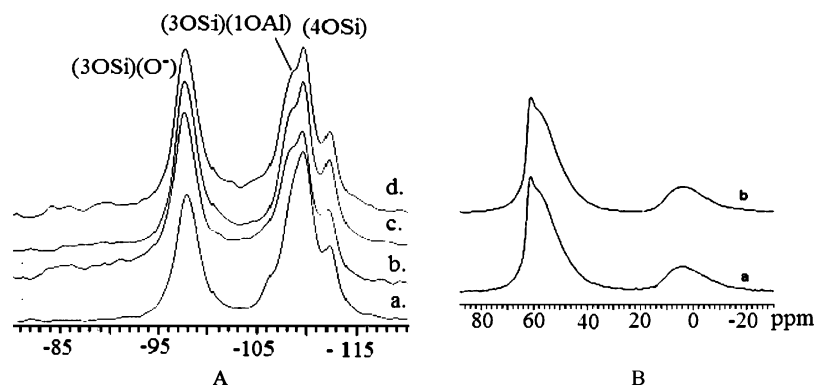


Figure 3. (A) Solid-state ^{29}Si MAS H-decoupled NMR of (a) pure siliceous Na magadiite, (b) 15[Al] magadiite, (c) 30[Al] magadiite, and (d) 60[Al] magadiite. (B) Solid-state ^{27}Al MAS H-decoupled NMR of (a) 30[Al] magadiite sample and (b) the same sample exchanged in $0.1 \text{ mol}\cdot\text{L}^{-1}$ NaNO_3 solution.

and of 30[Al] magadiite samples. In panels A and B, the usual packing of plates is observed, creating individual 10–15 μm aggregates that are typical of Na magadiite.³⁷ Panel C shows 30[Al] magadiite, with similar morphology to Na magadiite. A closer look at one of these aggregates, Figure 2D, shows that the plates are very inhomogeneous in size and that some of them present a curved shape. It is seen

also that the presence of aluminum has made the plates thicker in the borders. This effect could also be caused by the fact that aluminum is introduced in the synthesis when probably the crystallization is advanced and therefore causes more uptake of silicon from the reaction mother liquor.

The decoupled ^{29}Si MAS NMR spectrum of pure magadiite (Figure 3A, curve a) showed two distinct signals at -112.6 and -109.9 ppm and two shoulders at -106 and -109 ppm assigned to Q^4 [$\text{Si}(4\text{OSi})^{38}$] sites. A peak corresponding to Q^3 sites [$\text{Si}(3\text{OSi})(\text{O}^-)^{39}$] was observed at -98.1 ppm. After the addition of aluminum, the decoupled

(35) Pál-Borbély, G.; Auroux, A. *Stud. Surf. Sci. Catal.* **1995**, *94*, 55.
 (36) Fudala, A.; Konya, Z.; Kiyozumi, Y.; Niwa, S.I.; Toba, M.; Mizukami, F.; Lentz, P.B.; Nagy, J.; Kiricsi, I. *Microporous Mesoporous Mater.* **2000**, *35–6*, 631.
 (37) Pastore, H. O.; Munsignatti, M.; Mascarenhas, A. J. S. *Clays Clay Miner.* **2000**, *48*, 224.

(38) Dailey, J. S.; Pinnavaia, T. J. *Chem. Mater.* **1992**, *4*, 855.

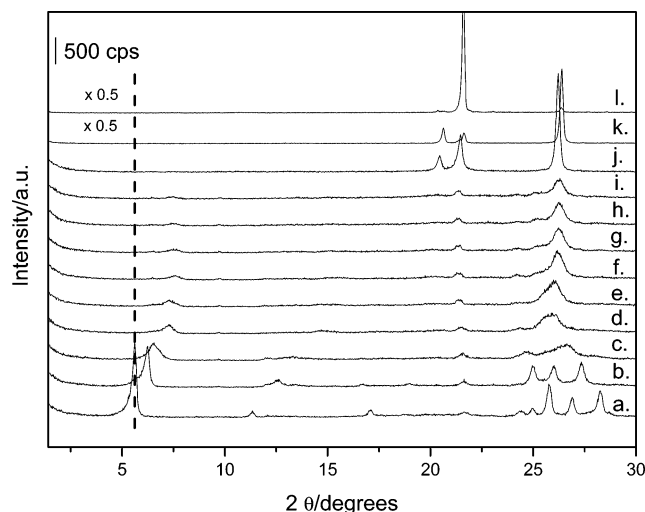


Figure 4. High-temperature in situ XRD of Na magadiite in air at (a) room temperature and at (b) 373, (c) 423, (d) 473, (e) 573, (f) 673, (g) 773, (h) 823, (i) 873, (j) 923, (k) 973, and (l) 1173 K.

^{29}Si MAS NMR of the Na[Al] magadiites (Figure 3A, curves b–d) shows signals at -112 and -109 ppm assigned to Q^4 Si(4OSi) and at -97 ppm due to Si[3OSi (O^-)] as commented for pure silica magadiite. The Q^3/Q^4 ratio increases in samples containing Al because the insertion of this element into the structure creates more silanol defects (see later). Another possibility is that the synthesis procedure can create more silanol sites due to the crystallization interruption for the introduction of the aluminum source.

A new and intense band appears at -108 ppm that is related to the presence of the aluminum ions in the framework, as already observed for kanemite.³³ The proximity of this band to the one corresponding to Si(4OSi) makes the evaluation of its total intensity difficult and not reliable. Due to the appearance of this band, the one at -106 ppm, noted for magadiite, is not observed anymore.

The proton-decoupled ^{27}Al MAS NMR spectra for these [Al] magadiite samples presented two main signals at 4.7 and 60.9 ppm assigned to aluminum species in octahedral and tetrahedral coordination,³⁵ respectively (Figure 3B).

The peak at 60.9 ppm presents a shoulder at approximately 57 ppm that is not an effect of the quadrupolar nucleus. This effect was seen before in MCM-22 and was attributed³⁸ to the presence of two types of aluminum sites. This is also the case for [Al] magadiite as will be discussed later. Ion-exchange procedures did not affect the ^{27}Al NMR profile (Figure 3B, curve b), indicating that the signal at 0 ppm is not due to cationic species trapped in the interlayer space.

1. Thermal Behavior of Purely Siliceous Na and NH_4 Magadiite. Figure 4 shows the results of in situ X-rays diffraction experiment at increasing temperatures and at ambient pressure. The most evident changes in the diffractograms, upon increasing the temperature to 373 K (Figure 4, curve b), that is, after water removal, are (i) a large decrease in intensity of a signal at $5.68^\circ 2\theta$ (1.55 nm) and its displacement to $6.24^\circ 2\theta$ (1.17 nm), (ii) an increase in intensity of a peak at $24.96^\circ 2\theta$, (iii) a disappearance of a

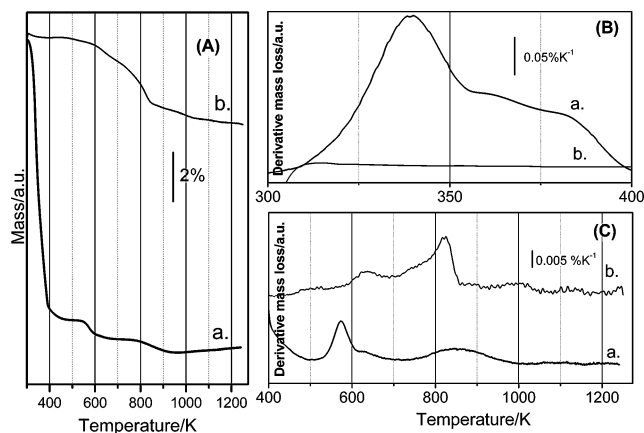


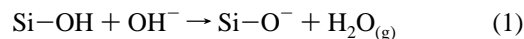
Figure 5. (A) Thermogravimetry and (B, C) differential thermogravimetry of (a) Na magadiite and (b) NH_4 magadiite. Data were collected under argon.

peak at $28.26^\circ 2\theta$, and (iv) a shift to 26.01° and $27.35^\circ 2\theta$ of peaks at 25.79° and $26.90^\circ 2\theta$ (these peaks change also in intensity). The diffraction at $5.68^\circ 2\theta$ is due to the (001) plane and corresponds to the interlayer distance, which gradually decreases upon increasing the temperature, reaching a value of 1.16 nm (corresponding to the signal located at $7.60^\circ 2\theta$) at 673 K (curves c–f).

The XRD results show that at 673 K (Figure 4, curve f) the interlayer distance has diminished by almost 0.4 nm, whereas other structural changes occur within the layer according to deep modifications of the pattern in the range 24 – $30^\circ 2\theta$, which become structureless, and a broad reflection at around $26.2^\circ 2\theta$ dominates the profile. Further increases in temperature, up to 873 K (curves g–i) do not cause deterioration of the Na magadiite structure. Only at 923 K (curve j) was a phase transition to quartz observed, and at 1173 K (curve l), a transition to cristobalite. These results indicate that the Na magadiite structure is thermally stable up to 873 K and that the layers become closer when water is released from the interlamellar space.

Figure 5 shows the thermogravimetry and differential thermogravimetry of Na magadiite (curves a) and NH_4 magadiite (curves b). As shown before,³⁹ Na magadiite shows three mass losses at low temperatures, 339, 362, and 382 K, due to the release of water loosely bound to other water molecules, in H-bond with silanoxo groups on the surface and bound to sodium ions, respectively. For Na magadiite, the total amount of water released at temperature below 400 K is ca. 13 wt %. Although the general appearance of the thermograms is similar, the temperatures of water release from Na magadiite observed in this work are slightly smaller than the ones indicated in the work of Eypert-Blaison et al.,³⁹ most probably because of the different measurement conditions. Beside pure dehydration at temperatures below 400 K, two well-defined weight losses were observed at 574 and 847 K, which were attributed to silanol's dehydroxylation of the magadiite framework with the formation of siloxane bonds. However, the IR results at variable temperature (vide infra) suggest that the weight loss from 500 to 600 K should be due to water release following the condensation of OH^- groups with silanols (eq 1):

(39) Eypert-Blaison, C.; Sauzéat, E.; Pelletier, M.; Michot, L. J.; Villieras, F.; Humbert, B. *Chem. Mater.* **2001**, *13*, 1480.



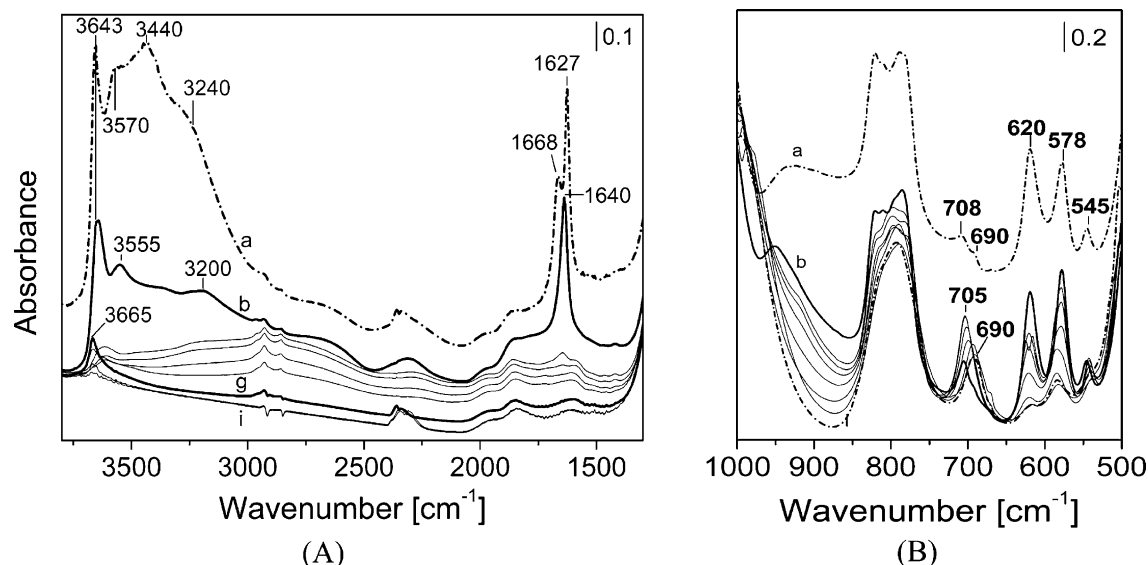
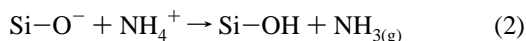


Figure 6. IR spectra collected at increasing temperatures of Na magadiite sample. Spectra are reported in the (A) 3800–1400 cm^{-1} and (B) 1000–500 cm^{-1} range: (a) spectrum in air at room temperature, and spectra in vacuum at (b) rt and at (c) 373, (d) 473, (e) 548, (f) 573, (g) 598, (h) 773, and (i) 873 K.

Replacement of Na^+ ions by NH_4^+ groups leads to a deep modification of hydration capability of the sample. As evidenced by TG data (Figure 5A,B, curve b), NH_4^+ magadiite contains a much lower amount of water with respect to the parent Na^+ magadiite, as expected from the strong decrease of Na^+ ions concentration in interlamellar position (see Table 2) due to ammonium exchange. Very weak signals are seen above 600 K range (Figure 5C, curve b) and are assigned to decomposition of NH_4^+ within the layers of NH_4 magadiite following reaction 2.

It is of note that the weight loss at 574 K of the Na magadiite sample is approximately the same as the sum of weight losses between 600 and 800 K of NH_4 magadiite sample, thus suggesting, in agreement with reactions 1 and 2, an almost quantitative substitution of Na^+ with NH_4^+ ions during the exchange procedure of Na magadiite:



These results are also confirmed by chemical analysis (Table 2), indicating that even though the $\text{Na}^+/\text{NH}_4^+$ ion exchange is not complete, the remaining amount of Na^+ ions is significantly lower (at least 1 order of magnitude) for the NH_4 magadiite sample in comparison to the parent samples.

Finally, a weight loss in the 800–900 K region was found for the NH_4 magadiite sample that can be assigned, in agreement with variable-temperature IR results (vide infra), to silanol nests⁴⁰ that are almost absent in the Na magadiite sample.

Figure 6 shows IR spectra of Na magadiite collected at increasing temperatures. The IR spectrum of Na magadiite in air at rt (Figure 6A, curve a) shows a broad absorption in the 3800–3000 cm^{-1} range, in which some overlapped components emerge as well-defined peaks located at 3643, 3570, 3440, and 3240 cm^{-1} . Broad absorptions in the 2800–2000 cm^{-1} range, located at ca. 2650 and 2310 cm^{-1} , are

also observed in the fully hydrated Na magadiite spectrum. In addition, narrow and intense bands at 1668 and 1627 cm^{-1} , with a shoulder at around 1640 cm^{-1} , are also present.

The bands between 3800 and 3150 cm^{-1} are due to the stretching modes of water molecules adsorbed on the Na magadiite surface, while the related bending modes fall at around 1600 cm^{-1} . In particular, the presence of the bands at 1668, 1627, and 1640 cm^{-1} (due to the δ_{OH} mode of different type of adsorbed water) are in good agreement with the results from thermogravimetry discussed above and with results reported in the literature, which indicate that Na magadiite contains different sites able to interact with water.⁴¹

The spectra of Na magadiite are also reported in the frequency region between 1000 and 500 cm^{-1} (Figure 6B), where the vibrations characteristic of the magadiite framework are found. According to literature data, the spectra in this region can be divided in three parts. In the spectrum of Na magadiite in air (Figure 6B, curve a), in the first part a band at ca. 950 cm^{-1} , due to the asymmetric stretching modes of terminal Si–OH interacting with water, is observed.⁴¹ In the second region (850–650 cm^{-1}), two main absorptions located at 820 and 790 cm^{-1} appear overlapped in an intense band that should be assigned to symmetric stretching modes of Si–O–Si groups, predominantly involving silicon motions [hereafter named as $\nu'(\text{Si-O-Si})$].^{42,43} Two very weak bands, which are assigned to the symmetric stretching vibration of Si–O–Si groups (resulting from a coupling of Si–O stretching motions, as indicated in ref 45), are also found at 708 and 690 cm^{-1} . Finally, in the third region (650–500 cm^{-1}) the bending modes of single and double Si–O–Si rings⁴⁵ are observed at 620, 578, and 545 cm^{-1} .

The intensity of the bands in the 3800–3000 cm^{-1} range decreased upon simple outgassing at rt (Figure 6A, curve

[41] Legrand, A. P. *The surface properties of silica*; John Wiley & Sons: New York, 1999; p 195.

[42] Laughlin, R. B.; Joannopoulos, J. D. *Phys. Rev. B* **1977**, *16*, 2942.

[43] Huang, Y.; Jiang, Z.; Schwieger, W. *Chem. Mater.* **1999**, *11*, 1210.

[44] Laughlin, R. B.; Joannopoulos, J. D. *Phys. Rev. B* **1977**, *16*, 2942.

[45] Rojo, J. M.; Ruiz-Hitzky, E.; Sanz, J. *Inorg. Chem.* **1988**, *27*, 2785.

[40] Zecchina, A.; Bordiga, S.; Spoto, G.; Marchese, L.; Petrini, G.; Leonfanti, G.; Padovan, M. *J. Phys. Chem.* **1992**, *96*, 4991.

b). This effect is particularly evident for the component at 3440 cm^{-1} . The outgassing procedure at rt also results in an evident modification of the bands at 1668 and 1627 cm^{-1} , which merge in a single peak at 1640 cm^{-1} . These results indicate that a significant amount of water molecules are very weakly bound to the magadiite surface and are simply removed by evacuation at rt. Water removal does not result in structural changes of the magadiite structure, as indicated by XRD (not shown) and by the IR spectrum in the $1000\text{--}500\text{ cm}^{-1}$ (Figure 6B, curve b). Nevertheless, such a dehydration leads to an intensification of the band at 708 cm^{-1} (which shifts to 705 cm^{-1} upon water removal) and is parallel to a decreasing of the interlayer space of the magadiite, as observed by XRD under air (not shown). Variable-temperature X-ray diffractograms taken under vacuum (data not shown for the sake of brevity), under conditions similar to those adopted for FTIR measurements, confirmed that the interlayer space decreased, from 1.57 to 1.49 nm , upon water removal at rt.

Some authors proposed that the 705 cm^{-1} absorption results from a coupling of stretching vibrations of free $[\text{SiO}_4]$ moieties, originating as two sets of stretching vibrations, both described by the stretching motions of adjacent Si–O bonds linked to the oxygen. In general, the $\nu_{\text{as}}(\text{Si–O–Si})$ stretching mode falls in the $1200\text{--}1000\text{ cm}^{-1}$ region, while the $\nu_{\text{s}}(\text{Si–O–Si})$ mode appears in the $700\text{--}400\text{ cm}^{-1}$ region.⁴⁵ The vibrational modes near 800 cm^{-1} are associated with a $\nu_{\text{s}}(\text{Si–O–Si})$ stretching vibration, especially involving silicon motion.⁴⁴ However, the considerable lowering of frequency of the Si–O–Si stretching vibration, normally found at ca. 800 cm^{-1} in silicates, cannot be explained only on the basis of coupling phenomena between $[\text{SiO}_4]$ tetrahedra. The downward shift of wavenumber up to ca. 700 cm^{-1} might also be due to the formation of rings by connection of $[\text{SiO}_4]$ entities of adjacent silicate layers of magadiite. As a matter of fact, these vibrations are found at intermediate positions between the symmetric Si–O–Si stretching vibrations (ca. 800 cm^{-1}) and the ring bending modes ($650\text{--}500\text{ cm}^{-1}$).

As described above, the appearance of the band at 705 cm^{-1} is strongly related to the hydration level of the sample and is induced to some extent by desorption of water molecules and approximation of magadiite layers. Indeed, desorption of water at relatively low temperature should result in a partial dehydroxylation of magadiite structure with consequent formation of silica rings, whose dimensions are not yet clear.

Upon heating of the sample at 373 K (Figure 6A, curve c), a decrease of the bands at 3643 , 3555 , and 3200 cm^{-1} occurs, along with a strong diminution of the broad signal in the $3800\text{--}3000\text{ cm}^{-1}$ region. At this stage, a broad absorption between 3500 and 2000 cm^{-1} is clearly evident, and weak bands at ca. 3615 and 1640 cm^{-1} are observed. The dehydration process at 373 K produces some modifications of the bands located at low frequencies. In particular, those at 820 and 790 cm^{-1} [related to $\nu'(\text{Si–O–Si})$ modes] decreased in intensity, together with the bands at 620 , 578 , and 545 cm^{-1} , due to bending vibrations of silica rings. This behavior is probably associated with local modifications occurring when dehydration processes take place. Conversely, the band at 705 cm^{-1} is intensified upon evacuation

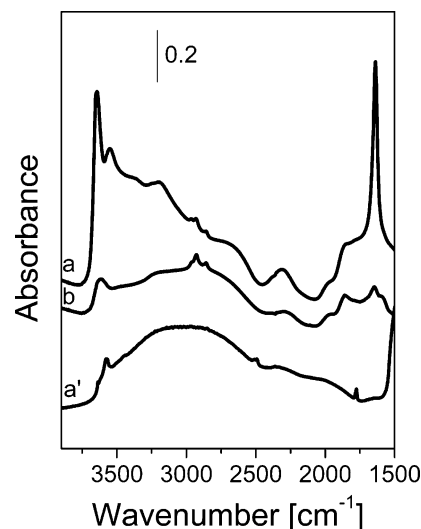


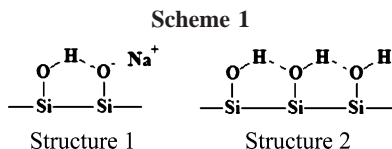
Figure 7. IR spectra of Na magadiite after outgassing at (a) room temperature and (b) 373 K for 30 min each, and (a') NaOH pellet (diluted in KBr) collected after outgassing at rt for 30 min.

at 373 K , and this is probably favored by the condensation of silanol groups and elimination of water, which allowed further coupling between adjacent silica layers.

The assignment of bands in the $3500\text{--}2000\text{ cm}^{-1}$ region needs additional comments. The absorptions in this region can be associated with vibrations of OH^- groups either solvated by water molecules or H-bonded to silanols within the interlamellar space. Clear-cut evidence of the presence of OH^- species in Na magadiite is found by comparison of the IR spectra of Na magadiite and of NaOH pellet (appropriately diluted in KBr powder) at different hydration levels (Figure 7). Figure 7 shows that the spectra of hydrated Na magadiite display absorptions typical of H-bonded OH^- species. Indeed, the broad bands in the $3500\text{--}2000\text{ cm}^{-1}$ range are very similar in partially dehydrated Na magadiite and NaOH samples (Figure 7, curves b and a'). As a matter of fact, these absorptions are not found in the IR spectra of NH_4 magadiite sample (vide infra) where OH^- species are not present. The presence of such alkali species was already suggested by Rojo et al.⁴⁵ by a combined SS NMR and IR study that proposed the formation of such additional phase during the synthesis in alkaline medium.

Nevertheless, recent computational and experimental results obtained on layered RUB-18 silica suggested that the observed double-hill profile observed in the $3500\text{--}2000\text{ cm}^{-1}$ range of fully or partially hydrated Na magadiite IR spectrum should be associated with a Fermi resonance phenomenon occurring between fundamental O–H stretching and overtone or combination modes of O–H species vibrating at low frequencies. These spectroscopic features should be related to the presence of a silanol hydrogen bridge, in which a proton is bound to two almost equivalent negatively charged oxygen atoms, as suggested by Gies and co-workers.⁴⁶ Further studies are in progress to elucidate this hypothesis.

If one continues to increase the temperature of the Na magadiite sample up to 873 K (Figure 6, curves d–i), a progressive decrease in the intensity of bands in the $3800\text{--}1500\text{ cm}^{-1}$ range is observed and is accompanied by the



parallel formation of a band located at 3665 cm^{-1} , which becomes particularly evident after heating of the sample at 598 K. At that temperature, a large part of OH^- species condense with silanols, releasing water molecules (see reaction 1), as shown by TG analysis (Figure 5A,C, curve a). The absorption at 3665 cm^{-1} is due to the presence of weakly perturbed terminal Si-OH groups on the silica surface remaining from the dehydroxylation process. In addition, three components at 1965, 1850, and 1600 cm^{-1} , due to combination and/or overtones of the silica framework,⁴⁷ remain after dehydration of the sample.

The nature of the perturbation of the silanols absorbing at 3665 cm^{-1} merits further discussion. After dehydroxylation and OH^- removal from the interlayer space (e.g., from the silica surface) the only remaining species are Si-OH , Si-O^- (on the silica surface), and Na^+ (in the interlayer space). It may be therefore proposed that silanols interact with vicinal Si-O^- groups (Scheme 1, structure 1) leading to a frequency shift of around 85 cm^{-1} in comparison to isolated groups, which absorb at ca. 3750 cm^{-1} in silicas.⁴⁸ The Si-O^- groups in this case behave as weak bases in that the oxygen negative charges are balanced by Na^+ ions. However, the presence of silanol nests similar to those found in defective silicalites, where multiple H-bonds may occur (Scheme 1, structure 2), cannot be discarded as their frequencies fall in the range $3700\text{--}3400\text{ cm}^{-1}$, the position being dependent on the hydroxyls' structure (i.e., on the charge density of both oxygen and hydrogen).

The band at 3665 cm^{-1} is not stable to heating procedures at higher temperatures and is progressively eroded until its disappearance at 873 K as a consequence of the condensation of remaining SiOH groups on the surface of the silicate layers, as discussed in relation to the thermogravimetry above.

Progressive heating at higher temperatures also results in strong modifications of the IR spectra in the $1000\text{--}500\text{ cm}^{-1}$ region: from 473 to 873 K (Figure 6A, curves d–i), the band at 705 cm^{-1} progressively shifts to lower frequency, being finally located at 690 cm^{-1} .

Moreover, the single/double rings (bands in the $700\text{--}500\text{ cm}^{-1}$) also appeared to be irreversibly modified with the increasing temperature; some of them disappeared in the transition to quartz structure. These results are in good agreement with XRD data and are indicating that as a consequence of the progressive heating the magadiite structure appears strongly modified, collapses, and undergoes phase transition to quartz and finally to cristobalite. The presence of Na^+ ions, which act as a mineralizing agent for silicates, may also catalyze the transformation from the magadiite structure to quartz and cristobalite, which show weak Si-OH surface groups. This point will be further discussed later in the text.

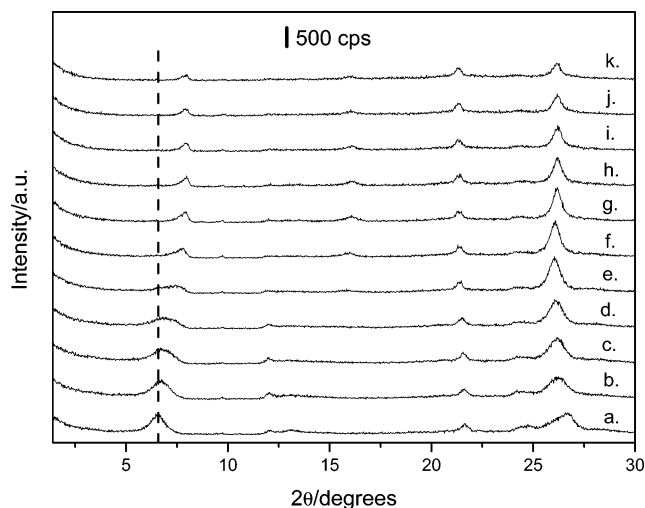


Figure 8. High-temperature in situ XRD of NH_4 magadiite at (a) room temperature and at (b) 373, (c) 423, (d) 473, (e) 573, (f) 673, (g) 773, (h) 873, (i) 973, (j) 1073, and (k) 1173 K.

The ion exchange of Na magadiite by ammonium causes important changes in the thermal properties of the sample. Figure 5, curves b, display the results. The presence of a lower amount of sodium in NH_4 magadiite with respect to Na magadiite makes the ammoniated sample more hydrophobic: the mass loss up to 473 K is only 1%, exceedingly lower than in Na magadiite. Also, the three distinct weight losses observed in the Na magadiite differential thermogravimetry (DTG) curve (Figure 5B, curve a) were replaced by a large unresolved weak signal (Figure 5B, curve b) at ca. 370 K. Weak DTG signals were observed at 635, 700–800 (unresolved), and 823 K. The first two signals are assigned in this work, by comparison with Na magadiite and $\text{NH}_4\text{-[Al]}$ magadiites (see later), to the release of ammonia. However, the second signal at 700–800 K may be also due to dehydroxylation processes that occur in this range of temperature. The signal at 823 K was undoubtedly assigned to dehydroxylation. Nevertheless, through a combination of TGA and variable-temperature IR analysis, a clearer indication of phenomena occurring in the NH_4 magadiite sample in the 600–1000 K temperature range will be given (see later).

Figure 8 displays high-temperature in situ XRD results obtained for NH_4 magadiite. Comparing the XRD profiles of Na and NH_4 magadiites at room temperature allows some immediate observations. The region between 24° and 30° 2θ (0.371 and 0.298 nm) is transformed from five narrow signals (Figure 4, curve a) to two wide and weak peaks (Figure 8, curve a). This suggests that the ion exchange of Na^+ with NH_4^+ perturbs short distance organization within the lamella. In the small-angle region of the diffractogram, the (001) diffraction appears at 6.50° 2θ (1.26 nm) instead of 5.68° , corresponding to a decrease of 0.31 nm of the basal distance, probably caused by the hydrophobic character of NH_4^+ magadiite, which retains a smaller amount of water in the interlayer space, as discussed before in relation to the DTG results. As a matter of fact, the NH_4 magadiite diffractogram at room temperature resembles very much the profile of Na magadiite at 423 K (Figure 4, curve c), where it has lost the hydration water.

(47) Benesi, H. A.; Jones, A. C. *J. Phys. Chem.* **1959**, *63*, 179.

(48) Ghiotti, G.; Garrone, E.; Morterra, C.; Bocuzzi, F. *J. Phys. Chem.* **1979**, *83*, 2863.

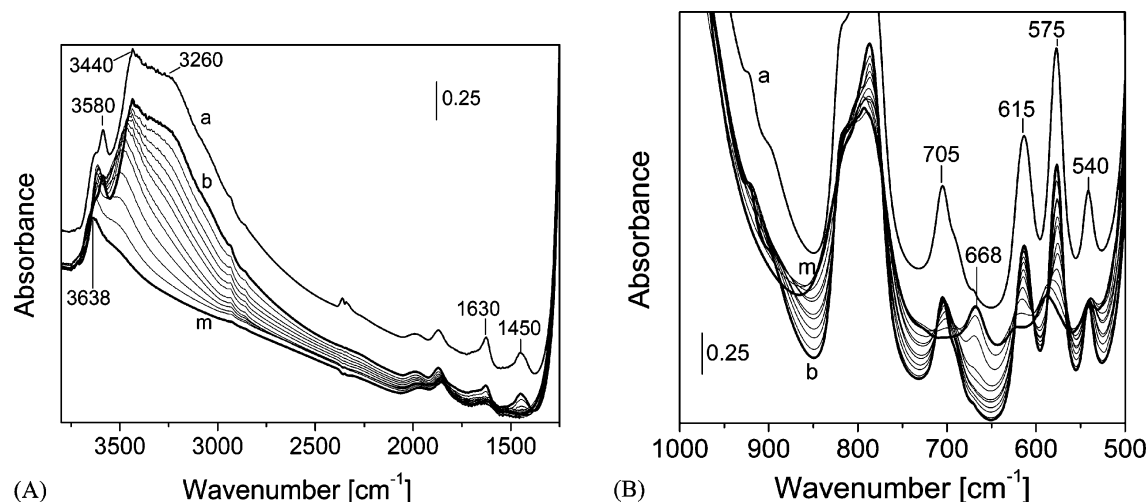


Figure 9. IR spectra collected after outgassing NH_4 magadiite sample at increasing temperature (from room temperature to 873 K). Spectra are reported in the (A) 3800–1400 cm^{-1} and (B) 1000–500 cm^{-1} range: (a) spectrum in air at rt, and spectra in vacuum at (b) rt and (c) 323, (d) 423, (e) 473, (f) 523, (g) 573, (h) 623, (i) 673, (j) 723, (k) 773, (l) 823, and (m) 873 K.

Heating the NH_4 magadiite at increasing temperatures causes the displacement of the (001) diffraction to $7.96^\circ 2\theta$ (1.11 nm, maximum displacement occurring at 773 K), a decrease of 0.15 nm of the basal space in relation with the same material at room temperature. At this point, NH_4 magadiite has been dehydrated and deammoniated, becoming the silicic acid H magadiite. Differently from Na magadiite, heating to even higher temperatures does not cause collapse of the H magadiite structure up to 1173 K, although the adsorptive properties dramatically changes (*vide infra*). The absence of sodium ions, which act in this case as mineralizing agent, has made the structure more thermally stable.

Figure 9 shows in situ IR spectra of NH_4 magadiite heated from rt to 873 K. The IR spectrum of the sample in air (Figure 9A, curve a) shows a large band in the high-wavenumber region (3800–3000 cm^{-1}) with maxima at 3580, 3440, and 3260 cm^{-1} , accompanied by two much weaker and narrower bands located at 1630 and 1450 cm^{-1} .

In the low-frequency range (1000–500 cm^{-1}) the spectrum of hydrated NH_4 magadiite (Figure 9B, curve a) appears very similar to that of dehydrated Na magadiite described above (Figure 6B, curve c). It is of note that in this case the 705 cm^{-1} band appears well-defined and more intense in comparison to the spectrum of Na magadiite sample collected in the same conditions. This behavior should be associated with the different hydration degrees of the magadiite samples. Indeed, as found by TG analysis, the exchange of Na^+ cations with NH_4^+ strongly influences the capability of the magadiite surface to adsorb water molecules.

The very low concentration of adsorbed water in the NH_4 magadiite sample can be inferred by the fact that the band at 1630 cm^{-1} of the water bending mode is very weak. The stretching modes of such adsorbed molecules contribute to the formation of a band at ca. 3580 cm^{-1} in the high-frequency range of the spectrum. However, the complex spectral pattern observed in the spectrum of NH_4 magadiite in the 3800–2500 cm^{-1} region (Figure 9A, curve a) is mainly due to the stretching modes of ammonium groups H-bonded to the magadiite silicate surface. The comparison of these results with those reported in literature⁴⁹ suggests that NH_4^+

groups are probably stabilized as multidentate complexes on the surface of the negatively charged silica layers. The presence of NH_4^+ groups is also evidenced by the characteristic band at 1450 cm^{-1} , due to a bending mode of ammonium ions.

Upon heating the NH_4 magadiite from rt to 873 K, the following behavior can be noticed: (i) the broad band at 3800–3000 cm^{-1} is progressively eroded and bands at higher wavenumber become more evident, (ii) the band at 1450 cm^{-1} disappears along with the band at ca. 3200 cm^{-1} , (iii) the 3660 cm^{-1} band shifts smoothly to 3670 cm^{-1} and the one at 3460 cm^{-1} shifts to 3490 cm^{-1} , and (iv) the band at 1450 cm^{-1} is essentially absent at 623 K under vacuum. This latter point suggests that deammoniation is almost complete at 623 K, deammoniation completely occurs for NH_4 magadiite sample, and from this fact the weight loss at ca. 600 K (see Figure 5) can be safely assigned to NH_4^+ decomposition. Spectra collected at 623 K, however, still show the presence of significant amounts of H-bonded silanol species. Dehydroxylation process of such species continue up to 900 K, as suggested by TGA results (Figure 5).

The broad bands in the 3500–3200 cm^{-1} range related to OH^- groups found in the spectra of Na magadiite are absent in the spectra of NH_4 magadiite, thus supporting the assignment proposed and reactions 1 and 2, which describe the evolution of the surface species of the two samples under heating. In the low-frequency region, 1000–500 cm^{-1} , little changes occurred up to 623 K. As noted above, in this region, the spectrum of NH_4 magadiite in air (Figure 9B, curve a) resembles that of the Na magadiite after evacuation at 373 K (Figure 6B, curve c), that is, when water is almost completely removed from the interlamellar space (which becomes smaller), and this follows the same trend found by XRD (*vide supra*). In particular, the presence of the band at 705 cm^{-1} in the spectrum of the NH_4 magadiite sample in air is probably caused by the closer proximity of the magadiite layers, which allows a stronger interaction between them, and also the lower amount of water present in the

(49) Zecchina, A.; Marchese, L.; Bordiga, S.; Pazé, C.; Gianotti, E. *J. Phys. Chem. B* 1997, 101, 48.

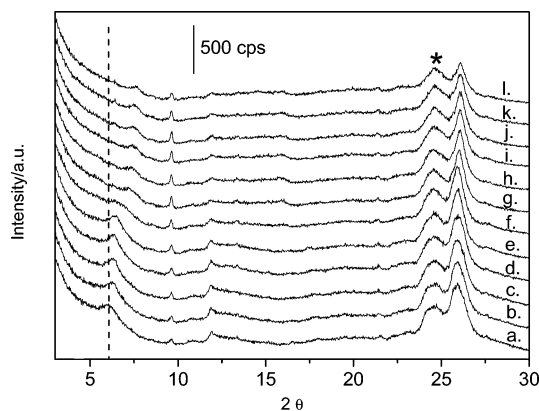


Figure 10. In situ XRD at variable temperatures of $\text{NH}_4[\text{Al}]$ magadiite with Si/Al molar ratio of 30 at (a) room temperature and at (b) 373, (c) 423, (d) 473, (e) 573, (f) 673, (g) 773, (h) 823, (i) 873, (j) 923, (k) 973, and (l) 1173 K. Asterisk indicates sample holder.

sample as already discussed in relation to the TGA. The bands due to single and double rings at 615, 575, and 540 cm^{-1} are still present after heating to 623 K, showing that the structure of the magadiite layer is preserved at this temperature as found by XRD. Two very weak bands are found at 900 and 925 cm^{-1} in the spectra of hydrated sample that can be assigned to Si–O stretching of Si–OH groups H-bonded to water molecules.⁴³

Summarizing, water molecules are embedded within the interlamellar space of Na and NH_4 magadiite samples in different concentrations and are bound to different sites within the solids. Water is released from Na magadiite and ammonia (along with a small amount of water) from NH_4 magadiite upon heating up to 593 K under vacuum. This causes the layers to approximate and form siloxane bridges along with silanols interact through H-bonding.

When dehydrated at 593 K, Na magadiite displays only one type of hydroxyl groups vibrating at 3665 cm^{-1} , which are associated with internal SiOH species weakly interacting by H-bonding (Scheme 1).⁴² Results collected after contact of the silica with D_2O indicated that such OH species are not exchanged into OD (spectra not shown for brevity) and for these reasons these type of silanols are identified as bulky, internal, or localized in inaccessible positions.⁵⁰ By contrast, NH_4 magadiite after dehydration shows two different bands respectively located at 3638 cm^{-1} (more intense) and ca. 3500 cm^{-1} (broad and poorly defined), which can be related to chained (or nests of) silanol groups.⁴² The fact that dehydrated magadiite samples do not show isolated SiOH groups typically present on external surface of silicas is another strong indication of the proximity of the silica layers in the lamellar structure after water removal.

2. Thermal Behavior of $\text{NH}_4[\text{Al}]$ Magadiite. $\text{NH}_4[\text{Al}]$ magadiite samples were submitted to high temperatures while in situ X-ray diffraction was measured at room atmosphere. Since similar results were obtained on samples with different Si/Al ratios, for the sake of simplicity only data related to $\text{NH}_4[\text{Al}]$ magadiite with Si/Al ratio of 30 are shown (Figure 10).

XRD diffraction studies showed that the thermal stability of the structure is similar to that of NH_4 magadiite (Figure 8). It was thus inferred that the introduction of Al ions does not affect the stability of the silica layers and that this property is governed only by the presence of sodium ions. The interlamellar space varied from 15.5 to 14.8 Å by heating at 473 K, due to desorption of water molecules.

This process was also followed by TGA (Figure 11), which showed that $\text{NH}_4[\text{Al}]$ magadiites contained a much lower amount of water with respect to Na magadiite, as expected

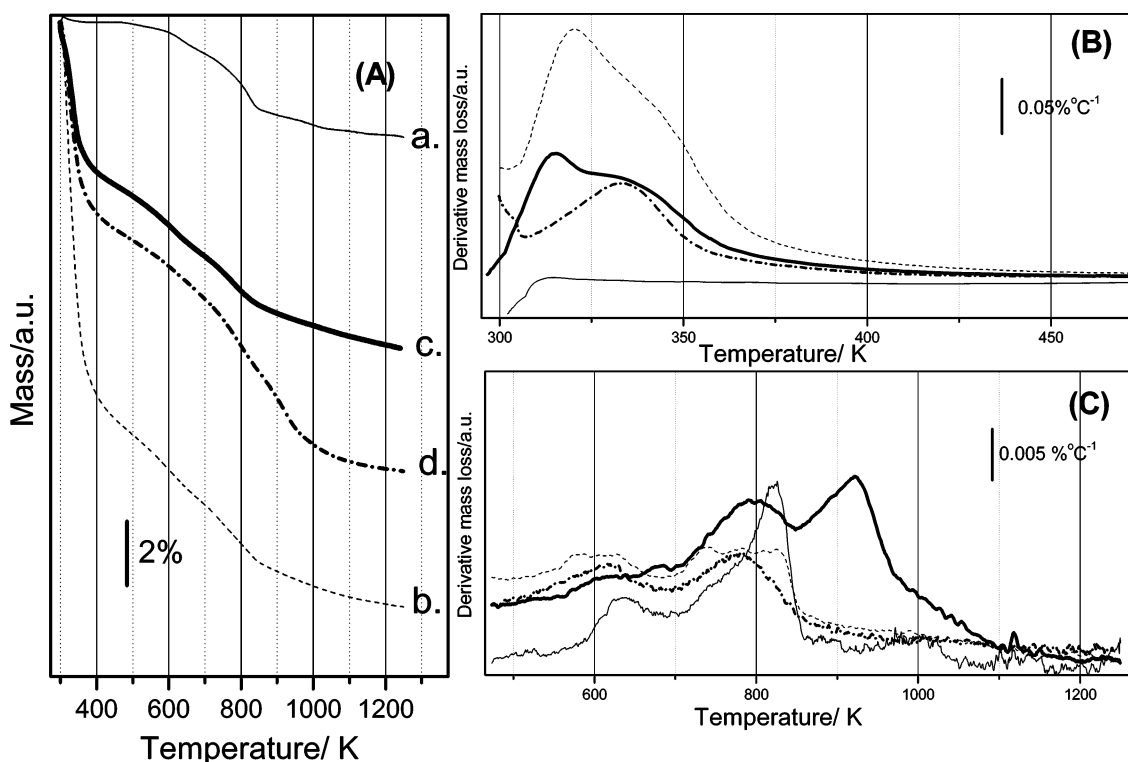


Figure 11. (A) Thermogravimetry and (B, C) derivative thermogravimetry of (a) NH_4^+ magadiite and of $\text{NH}_4^+[\text{Al}]$ magadiite at Si/Al molar ratios of (b) 15, (c) 30, and (d) 60.

from the absence of Na^+ ions in interlamellar positions, but a higher concentration in relation to NH_4^+ magadiite. This is probably due to the fact that a larger number of ion-exchange sites are available in $\text{NH}_4[\text{Al}]$ magadiite.

The water release occurs in two temperatures for NH_4 -[Al] magadiite, the first one very close to NH_4 magadiite and the second one at around 332 K, which is more important in relation to the one at lower temperatures as the Si/Al ratio increases (Figure 11B). It has to be noticed that, conversely to what was found in the case of Na magadiite, weight loss at 350–400 K is almost absent in $\text{NH}_4[\text{Al}]$ magadiite samples.

At higher temperatures (Figure 11C), deammoniation is observed at around 600 K and dehydroxylation at approximately 800 K. The samples with less structural aluminum, which are more acidic, are more resistant to NH_3 release because the acceptance of H^+ by the framework is more difficult. Thus, while for $\text{NH}_4[\text{Al}]$ magadiite with Si/Al 15 and 30 the deammoniation reaction occurs below 600 K, for the sample with Si/Al 60 it takes place at temperatures slightly higher than 600 K. These results were confirmed by IR spectroscopy (data not shown for the sake of brevity).

FTIR spectra of NH_4 magadiite and $\text{NH}_4[\text{Al}]$ magadiite in the region characteristic of bending modes of adsorbed water and ammonium ions are displayed in Figure 12. Data reported in Figure 12 can be summarized as follows: (i) By increasing progressively the Al content in NH_4 magadiite samples, the amounts of ammonium species and adsorbed water (whose presence is indicated by bands centered at ca. 1460 and 1630 cm^{-1} respectively) increase. (ii) The removal of water in such samples occurs almost completely at rt, while for Na-containing sample a similar water amount is lost only after heating at 373 K (see Figure 6 described above). These IR data are in good agreement with TG results described above (Figure 11).

3. Surface Properties of Na Magadiite, $\text{NH}_4[\text{Al}]$ Magadiite, and $\text{H}[\text{Al}]$ Magadiite. Figure 13 shows the IR spectra, in the 3800–3000 cm^{-1} range, of Na magadiite (Figure 13, curve a), of NH_4 magadiite (Figure 13, curve b), and of $\text{NH}_4[\text{Al}]$ magadiites with Si/Al ratio of 60, 30, and 15 (Figure 13, curves c, d, and e, respectively). The spectrum of Na magadiite was discussed above (Figure 6).

The IR spectrum of NH_4 magadiite (Figure 13, curve b) appears very different from that of Na magadiite. In the 3800–3000 cm^{-1} range this spectrum is dominated by broad absorptions with maxima at 3620 and around 3470 cm^{-1} .

Similarly to what was found in highly defective silicalites, the bands at lower frequency between 3650 and 3200 cm^{-1} can be assigned to the OH stretching modes of hydrogen-bonded Si–OH groups.⁴² Zecchina et al.,⁵⁷ in fact, proposed that hydroxyl groups present at internal defects (or nests) are prevalently grouped together in chains that can have variable length and shape, depending on the structure of defects. The much lower amount of defects in Na magadiite is due to the fact that Na^+ ions balance the SiO^- groups, which are the sites that lead to silanols after ammonium exchange and thermal decomposition.

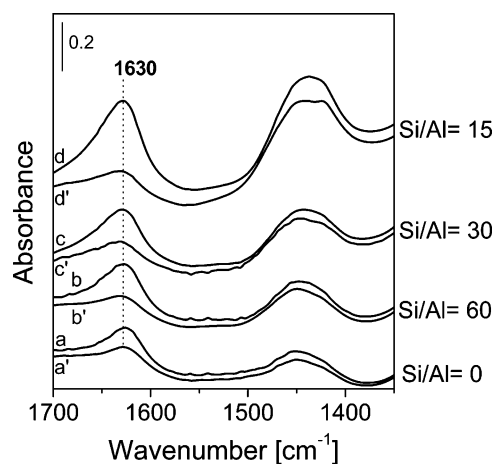


Figure 12. IR spectra of NH_4 magadiite (a, a') and $\text{NH}_4[\text{Al}]$ magadiite at Si/Al ratios of 60 (b, b'), 30 (c, c'), and 15 (d, d'), in air (unprimed) and after outgassing for 10 min (primed).

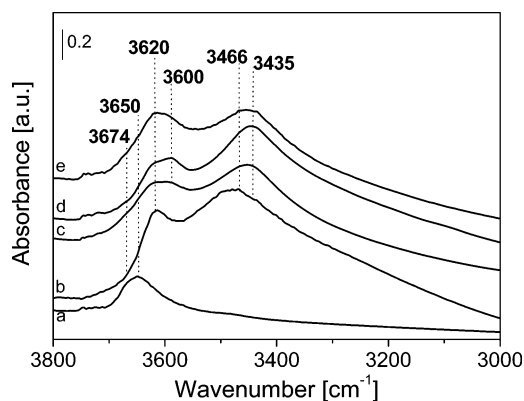


Figure 13. IR spectra, in the 3800–3000 cm^{-1} range, of (a) Na magadiite, (b) NH_4 magadiite, and $\text{H}[\text{Al}]$ magadiite with Si/Al ratio of (c) 60, (d) 30, and (e) 15 prepared from the in situ thermal decomposition of $\text{NH}_4[\text{Al}]$ magadiite described in the Experimental Section. All samples were outgassed at 350 °C for 3.5 h.

The addition of Al leads to modifications in the intensity and width of the IR spectrum of the $\text{NH}_4[\text{Al}]$ magadiite samples (Figure 13, curves c–e). Such spectra are dominated by two broad absorptions where bands at 3620, 3600, 3466, and 3435 cm^{-1} were identified by using the second-derivative curves of the related background-corrected spectrum (elaboration not shown for the sake of brevity). In addition, the bands characteristic of the pure magadiite located at ca. 3670 cm^{-1} are still observed in these samples, although they are heavily overlapped by the main absorptions at 3620–3600 cm^{-1} , due to hydrogen-bonded Si–OH groups,⁴² which are more abundant than those found in the Na magadiite (Figure 13, curve a).

Interestingly, the introduction of progressive amounts of Al (Si/Al ratio of 30 and 15) during the synthesis results in a modification of the relative intensities of the bands already observed in the sample with the lowest Al content. It is inferred that the preparation of [Al] magadiite leads to materials with a large amount of silanols in internal defects, or nests, in the silicate structure. The ^{27}Al MAS NMR data previously discussed indicated that the addition of aluminum leads to the incorporation of ions in the framework of pure siliceous magadiite. Following these indications, bands at around 3600 cm^{-1} in the case of [Al]-modified magadiite should be also related to the formation either of bridged Si–

(50) Davydov, V. Ya.; Zhuravlev, L. T.; Kiselev, A. V. *Russ. J. Phys. Chem. (Engl. Transl.)* **1964**, *38*, 1108.

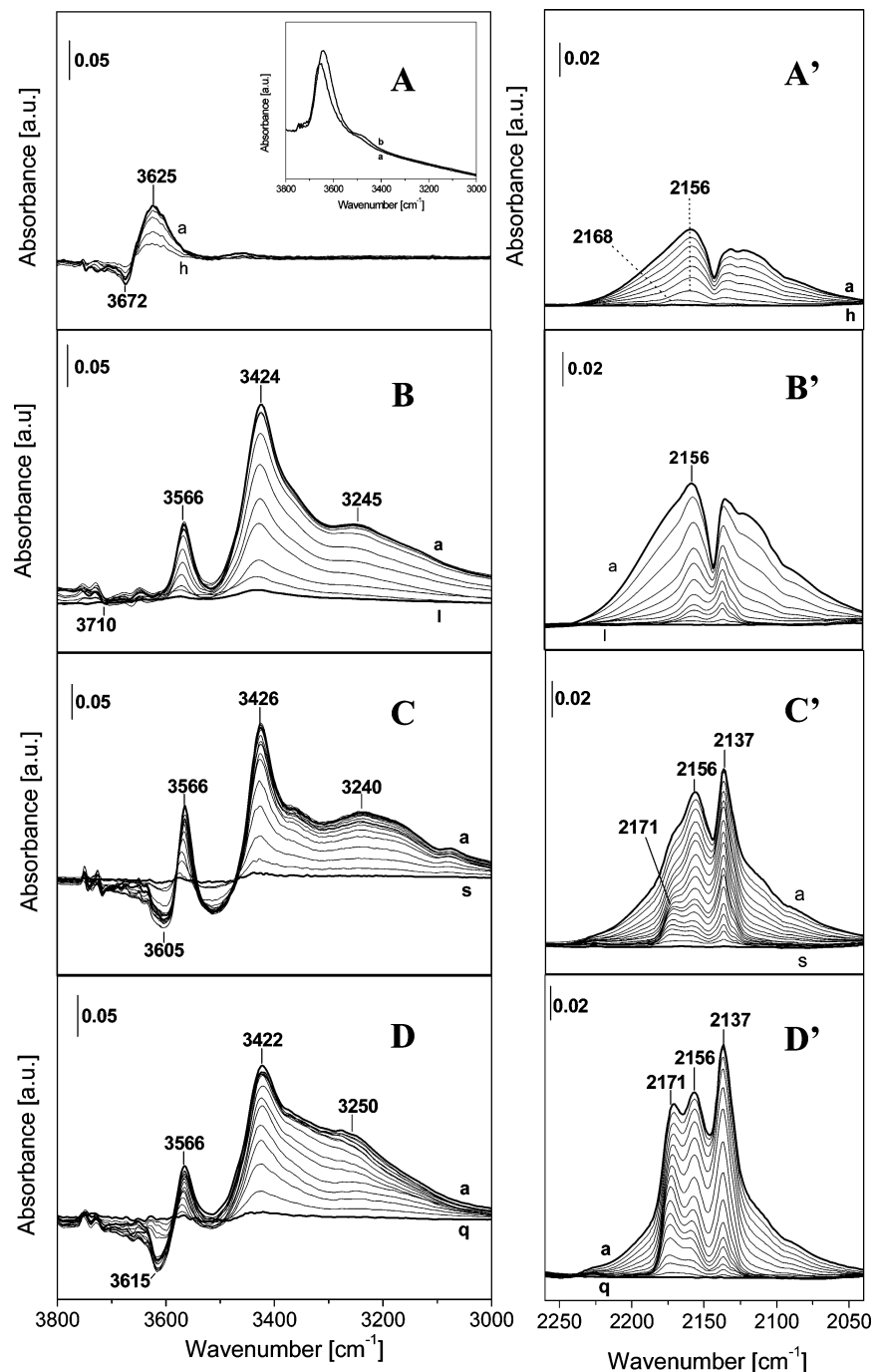


Figure 14. IR spectra of CO adsorption at 100 K (30 Torr) on (A, A') Na⁺ magadiite and on [Al] magadiite samples with Si/Al ratio of (B, B') 60, (C, C') 30, and (D, D') 15 outgassed at 350 °C for 3.5 h. (A–C Differential spectra in the 3800–3000 cm⁻¹ range; (A'–C') differential spectra in the 2225–2075 cm⁻¹ range obtained by subtracting, for each sample, the spectrum of the material before CO admission. Lettering is in the order of decreasing CO pressure.

(OH)Al species or of Al–OH groups, and this makes the identification more difficult.

The decomposition of ammonium ions in NH₄-exchanged magadiite and NH₄[Al] magadiite leads to Brønsted acid sites, which were monitored in this work by IR spectroscopy of CO adsorbed at 100K (Figure 14). It is well-known that the interaction of CO with hydroxyl groups in silicates and aluminosilicates is a powerful tool for monitoring their acidity.^{51,52} For this reason, IR of CO adsorbed at low

temperature was used in this work to give additional insights on the nature and strength of acid sites produced by addition of increasing amounts of Al in the silica magadiite framework.

Figure 14 displays the IR spectra collected upon decreasing CO coverage in Na magadiite (panels A and A'), used for comparison, and Al-derived magadiites with Si/Al ratio of 60 (panels B and B'), 30 (panels C and C'), and 15 (panels D and D'). Left-side panels (unprimed) show the spectra in the ν_{OH} region, while those on the right side (primed) show the spectra in the ν_{CO} region, reported after subtraction of the spectrum of the samples prior to CO adsorption as background.

(51) Sauer, J.; Ugliengo, P.; Garrone, E.; Saunders V. R. *Chem. Rev.* **1994**, *94*, 2095.

(52) Hadjiivanov, K. I.; Vayssilov, G. N. *Adv. Catal.* **2002**, *47*, 307.

In the case of Na magadiite, only a very small fraction of hydroxyls is perturbed by CO adsorption (as clearly shown in the inset of Figure 14A, which displays the absorption spectra before and after contact with maximum CO dose). The admission of 30 Torr CO causes the conversion of the Si–OH band peaked at 3672 cm^{-1} (negative band in Figure 14A) to a more intense absorption with maximum at 3625 cm^{-1} (Figure 14A, curve a); the wavenumber shift ($\Delta\nu_{\text{OH}}$) of 60 cm^{-1} found for these hydroxyls is similar to that found for amorphous silica.⁴⁹

Bands due to the two branches of the rotovibrational spectrum of CO in the gas phase, which are centered at 2143 cm^{-1} , dominate the spectra in the ν_{CO} stretching region (Figure 14A', curve a). Only two very weak absorptions, heavily overlapped with the CO gas absorption, were observed at 2168 and 2156 cm^{-1} (more evident at lower CO doses).

By decreasing the CO pressure, the 3625 cm^{-1} band progressively decreases, and it is converted into the original at 3672 cm^{-1} (Figure 14, curves b–h), along with a decrease of the bands in the CO stretching region. The absorption at 2156 cm^{-1} is associated with the stretching frequency of CO hydrogen-bonded to Si–OH species: very weak adducts are formed and their frequency value is only slightly higher than that of CO gas.⁵³ At very low CO coverage, an exceedingly weak band at 2168 cm^{-1} , due to CO polarized on Na^+ ions, appears.⁵³

CO adsorption on $\text{NH}_4[\text{Al}]$ magadiite sample with Si/Al ratio = 60 (Figure 14B, B–L) results in a partial erosion of the bands in the ν_{OH} stretching region discussed above (especially those in the $3750\text{--}3600\text{ cm}^{-1}$ range) and in the formation of different bands located at 3566 , 3424 , 3350 (shoulder), and $3250\text{--}3240\text{ cm}^{-1}$. The collected data indicate that, after interaction with CO at low temperature, a band at ca. $3750\text{--}3700\text{ cm}^{-1}$ is shifted to 3566 cm^{-1} ($\Delta\nu_{\text{OH}} = 184\text{--}134\text{ cm}^{-1}$), while absorptions in the $3650\text{--}3500\text{ cm}^{-1}$ range (minima at 3605 and 3510 cm^{-1}) give origin to well-defined bands located at 3426 and 3240 cm^{-1} , the associated $\Delta\nu_{\text{OH}}$ shifts being ca. $200\text{--}250$ and $300\text{--}350\text{ cm}^{-1}$. The appearance of such bands indicates that the addition of aluminum in the pure siliceous framework of magadiite results in the formation of sites able to give stronger interactions with CO, as witnessed by the observed higher $\Delta\nu_{\text{OH}}$ shifts. The complexity of the collected spectra is probably due to the presence of at least three different families of acid sites, characterized by different acid strengths. In particular, the OH groups vibrating originally at ca. $3750\text{--}3700\text{ cm}^{-1}$ cannot be assigned to SiOH species, for the $\Delta\nu_{\text{OH}}$ values upon CO adsorption are much larger ($\Delta\nu_{\text{OH}} = 184\text{--}134\text{ cm}^{-1}$ vs $90\text{--}60\text{ cm}^{-1}$). These species should be more probably Al–OH groups, which are more acidic than SiOH species. However, a detailed discussion concerning the assignments of bands formed upon CO adsorption in relation to the nature and strength of the original surface OH groups can be given only by taking into account the data collected on the complete series of samples containing increasing Si/Al ratios. The

absorptions in the ν_{OH} stretching region that appeared after CO adsorption are progressively converted into the original ones by decreasing the CO doses (Figure 14A, curves b–l), as observed for Na magadiite.

The spectrum of adsorbed CO in the ν_{CO} stretching region appears dominated by two bands at 2156 and 2137 (more intense) cm^{-1} . This last band (with a shoulder at 2110 cm^{-1}) is due to liquid-like CO condensed in the lamellar galleries of the magadiite structure.^{54,55} In addition, beside the broad tail characteristics of CO gas, a shoulder located at ca. 2170 cm^{-1} , probably associated with the stretching mode of CO adsorbed on Brønsted acid sites, is present.

In the case of the $\text{NH}_4[\text{Al}]$ magadiite with Si/Al of 30, adsorption of CO causes similar changes of the IR spectrum in the ν_{OH} stretching region as those observed for the sample with lower Al content (Figure 14C,C'). In this case, adsorption of CO results in a partial erosion of the 3605 cm^{-1} band (particularly evident in this sample) with consequent formation of bands at 3566 , 3426 , and 3240 cm^{-1} (Figure 14C, curve a). In the CO stretching region, besides the bands at 2156 and 2137 cm^{-1} (very intense), also a band at 2171 cm^{-1} appears. With decreasing CO pressure, the observed bands decrease in intensity (Figure 14C,C', curves b–s), and at a very low CO pressure ($p < 0.5$ Torr) a band at ca. 2165 cm^{-1} , initially hidden by the intense component at 2156 cm^{-1} , appears.

For the Al-richest sample, interaction with CO at low temperature leads to bands similar to those observed in the previous cases. However, a more intense 3250 cm^{-1} band (after CO interaction) is formed after erosion of the original band at 3615 cm^{-1} (Figure 14D, curve a). In addition, a broad band located at ca. 3350 cm^{-1} appears. This sample shows a very intense component at 2171 cm^{-1} , demonstrating that a high aluminum content corresponds to a higher concentration of bridged acid species (Figure 14D', curve a).

Bands in the ν_{OH} and ν_{CO} spectral regions decrease in intensity with decreasing CO coverage (Figure 14D,D', curves b–q). In particular, the stability of the component at 3350 cm^{-1} during evacuation appears lower with respect to the other bands, witnessing the presence of sites with different acid strength.

The collection of IR results dealing with CO adsorption reinforced the evidence of the presence of different families of Brønsted acid sites in $\text{NH}_4[\text{Al}]$ magadiite samples, especially at higher Al content. The different shifts upon interaction with CO reflect differences in their acid strengths that, in turn, should result from differences in their local structures.

These results indicate that, besides Al–OH species with weak acidity ($\Delta\nu_{\text{OH}} = 184\text{--}134\text{ cm}^{-1}$) discussed above, other acid groups should be present at the surface of [Al] magadiite samples. Indeed, strong acid sites ($\Delta\nu_{\text{OH}} = 300\text{--}350\text{ cm}^{-1}$), which might resemble the bridged Si(OH)Al species commonly found in zeolites, have been found in [Al]-modified materials. As a matter of fact, such a large shift is comparable

(53) Nakamoto, K. *Infrared and Raman Spectra of Inorganic and Coordination Compounds*, 3rd ed.; Wiley InterScience: New York, 1978; p 107.

(54) Ewing, G. E. *J. Chem. Phys.* **1962**, *37*, 2250.

(55) Jang, G. J.; Person, W. B.; Brown, K. G. *J. Chem. Phys.* **1975**, *62*, 1201.

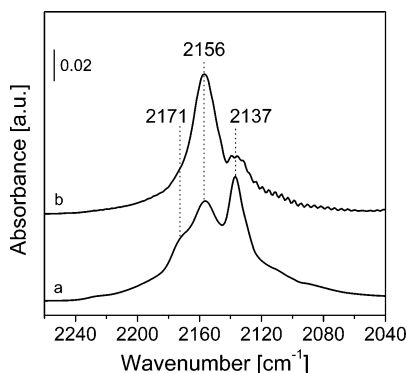


Figure 15. IR spectra of CO adsorbed at 100 K (20 Torr) in the 2260–2040 cm^{-1} range of (a) H[Al] magadiite and (b) H_{ex} [Al] magadiite with the same Si/Al ratio of 30. Prior to CO adsorption, NH_4 [Al] magadiite was outgassed at 623 K for 3.5 h, while the H_{ex} /Al magadiite sample was evacuated at 473 K for 2 h.

with that of highly acidic H mordenite zeolite ($\Delta\nu_{\text{OH}}$ between 359 and 389 cm^{-1}).⁵⁶

Sites characterized by medium acidity ($\Delta\nu_{\text{OH}} = 200\text{--}250$ cm^{-1}) are also present and should be interpreted as evidence of the presence of another family of Al–OH species in which Al is partially extraframework with a structure similar to those found in zeolites.⁵⁷

It must be underlined that the bands formed upon CO adsorption for Al-rich samples are found in very similar positions to those observed for acid zeolites (this is more evident in the ν_{CO} stretching region). Indeed, the band at 2171 cm^{-1} due to probe molecules adsorbed on Brønsted acid sites is slightly more stable with respect to the 2165 and 2156 cm^{-1} bands (related to CO adsorbed on extraframework Al–OH species and silanols, respectively) and to the 2137 cm^{-1} band (typical of liquid-like CO) (Figure 14C',D').

4. Monitoring the Accessibility of Acid Surface Sites of H^+ [Al] Magadiite by FTIR of CO Adsorbed at 100 K.

Data coming from comparison of the intensity of bands formed in the NH_4 [Al] magadiite samples with those collected on a H-BEA zeolite⁵⁸ with analogous Al content indicate that only ca. 10% of bridged Si(OH)Al sites in the [Al] magadiite case are available and accessible for the interaction with CO. In order to prove this hypothesis, two types of acid [Al] magadiite will be examined here: (1) the ones prepared by decomposition of NH_4 [Al] magadiite (H[Al] magadiite) and (2) H_{ex} [Al] magadiite sample, obtained by direct H^+ exchange of Na[Al] magadiite with HCl. Figure 15 displays the comparison between the IR spectra collected after admission of 20 Torr CO at 100 K on these samples. As described before (Figure 14), the admission of the highest CO dose at 100 K on H[Al] magadiite sample results in the formation of three main bands, located at 2171, 2156, and 2137 cm^{-1} , related to the stretching mode of CO H-bonded to acid Si(OH)Al groups and Si–OH species and physisorbed

CO condensed in the interlamellar space of magadiite structure, respectively (Figure 15, curve a).

Interestingly, the contact of H_{ex} [Al] magadiite with the same CO pressure sample leads to a different spectrum in comparison with the analogous sample exchanged with NH_4^+ . In particular, upon CO adsorption on H_{ex} [Al] magadiite sample (Figure 15, curve b), an intense band at 2156 cm^{-1} is formed while the bands at 2171 and 2137 cm^{-1} appear strongly decreased in intensity with respect to the case of H[Al] magadiite. In good agreement with chemical analysis, the band at 2171 cm^{-1} , assigned to CO interacting with Si(OH)Al species, appeared decreased in intensity in H_{ex} [Al] magadiite sample due to the lower Al content of this sample as compared to H[Al] magadiite. However, the strong reduction of the 2171 cm^{-1} band, due to liquid-like CO, might be also interpreted in terms of a reduced accessibility of H_{ex} [Al] magadiite sample with respect to H[Al] magadiite sample associated with a larger reduction of interlamellar space occurring after water removal. The limited accessibility to the interlayer space of the H_{ex} [Al] magadiite sample also explains the strong reduction of the 2137 cm^{-1} band due to liquid-like CO.

It may be proposed that the thermal dehydration of NH_4 magadiite is the first process occurring at increasing temperatures; thus the hydrated sample transforms to dehydrated NH_4 magadiite but still holds the magadiite layers apart, and therefore bonding between the layers is prevented. In the case of H_{ex} magadiite, the simple dehydration is going to allow the layers to approximate extensively and allows some bonding between them, thus closing spaces and reducing the accessibility to the interlayer space and to the acid sites. One reasonable measure of the difference in the interlayer space is the position of the (001) peak in the XRD of the dehydrated NH_4 [Al] magadiite in comparison to the dehydrated, deammoniated H[Al] magadiite, curves d and g of Figure 10. Calculation of the distances afforded 14.8 Å for dehydrated NH_4 [Al] magadiite and 11.8 Å for H[Al] magadiite.

Conclusions

In this paper, different hydrothermal methods for the introduction of Al ions in layered magadiite materials were proposed. XRD studies showed that a new aluminum-induced crystallization method allowed us to obtain high-purity Al-modified magadiite samples with variable Al concentration. The physicochemical features of these modified materials were studied by a combination of different experimental techniques (XRD, SS MAS NMR, FTIR spectroscopy of adsorbed probe molecules, TGA) in relation to those exhibited by siliceous magadiite materials.

²⁷Al-MAS NMR showed that aluminum induced crystallization appeared efficient for the introduction of Al ions tetrahedrally coordinated into the magadiite framework, even if a small fraction of octahedral species was also present.

Interestingly, SEM analysis showed that the morphology of the Al-modified samples is similar to that occurring in the siliceous materials, even if the presence of Al led to a general thickening of the border of the platelets. In addition, the thermal stability of the silicate layers of magadiite was

(56) Jang, M.; Karge, H. C. *J. Chem. Soc., Faraday Trans.* **1996**, *92*, 2641.

(57) Zecchina, A.; Bordiga, S.; Spoto, G.; Scarano, D.; Petrini, G.; Leonfanti, G.; Padovan, M.; Otero Areán, C. *J. Chem. Soc., Faraday Trans.* **1992**, *88* (19), 2959.

(58) Bisio, C.; Massiani, P.; Fajerweg, K.; Sordelli, L.; Stievano, L.; Silva, E. R.; Coluccia, S.; Martra, G. *Microporous Mesoporous Mater.* **2006**, *90*, 75.

not modified by the presence of framework Al species, as evidenced by variable-temperature XRD studies.

By contrast, the surface properties of Al-derived samples appeared significantly modified with respect to those of the siliceous parent, in that surface acid groups were generated by the introduction of Al ions in the magadiite framework. Indeed, FTIR spectroscopy of adsorbed CO at 100 K revealed the presence of surface acidity compared to that of the most acidic zeolites. The presence of zeolite-type sites, Si(OH)-Al, whose amount was strictly related to the Al concentration, was therefore inferred. Moreover, CO adsorption allowed a fine-tuning of the surface acidity and several families of Brønsted acid sites, characterized by different acid strength, were found. In particular, besides Brønsted Si(OH)Al hydroxyl species, also a significant amount of sites with medium surface acidity was found. The existence of such

hydroxyl groups was related to the presence of Al ions with partial extraframework character, similarly to other aluminosilicates.

The relative amounts of such different acid surface groups could be tuned by appropriate modification of the synthesis procedure, thus revealing the possibility to adapt these new materials for a large variety of applications.

Acknowledgment. We acknowledge financial support from the “Fundação de Amparo à Pesquisa no Estado de São Paulo, (FAPESP), from the European Commission (STABILIGHT STRP project), and from the Italian Ministero dell’Istruzione, dell’Università e della Ricerca (Internazionalizzazione project, Bando MIUR-PSU 2004-2006 art. 23, FIRB 2001 project).

CM0707657